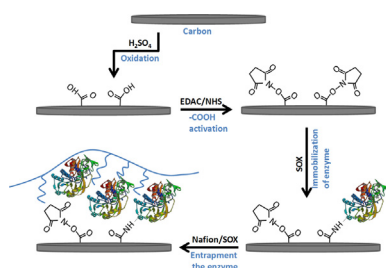


# Sarcosine oxidase composite screen-printed electrode for sarcosine determination in biological samples

Tânia S.C.R. Rebelo, Carlos M. Pereira, M.Goreti F. Sales, João P. Noronha, J. Costa-Rodrigues, Fernando Silva, M.H. Fernandes

## GRAPHICAL ABSTRACT



## ABSTRACT

As the prostate cancer (PCa) progresses, sarcosine levels increase both in tumor cells and in urine samples, suggesting that its metabolite measurements can help in the creation of non-invasive diagnostic methods for this disease. In this work, a biosensor device was developed for the quantification of sarcosine via electrochemical detection of  $H_2O_2$  (at 0.6 V) generated from the catalyzed oxidation of sarcosine. The detection was carried out after the modification of carbon screen-printed electrodes (SPEs) by immobilization of sarcosine oxidase (SOX) on the electrode surface. The strategies used herein included the activation of the carbon films by an electrochemical step and the formation of an NHS/EDAC layer to bond the enzyme to the electrode, the use of metallic or semiconductor nanoparticles layer previously or during the enzyme immobilization. In order to improve the sensor stability and selectivity, a polymer layer with extra enzyme content was further added. The proposed methodology for the detection of sarcosine allowed obtaining a limit of detection (LOD) of 16 nM, using a linear concentration range between 10 and 100 nM. The biosensor was successfully applied to the analysis of sarcosine in urine samples.

### Keywords:

Sarcosine  
Sarcosine oxidase  
Electrochemical biosensor  
Screen-printed electrodes  
Urine

## 1. Introduction

Prostate cancer (PCa) is the most common form of cancer in men in Europe with a 61.4% incidence among all cancer cases and a 12.1% mortality [1] and, therefore, its early detection is fundamental for increasing the survival rate. Currently, diagnosis and management of patients with PCa is only based on the

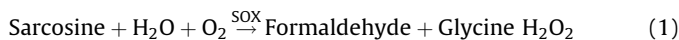
determination of the biomarker prostate specific antigen (PSA). In biological samples (urine and blood plasma) sarcosine concentration can range between 1 and 20  $\mu\text{M}$  [2]. However, the method used for PCa detection has poor sensitivity and specificity, leading to false-negative and false-positive test results and therefore, many patients are sent to unnecessary biopsy procedures [3]. Therefore, there is a need to seek for new biomarkers and more effective screening.

In 2009, a pilot study created a non-invasive method to identify the presence and aggressiveness of PCa disease, which was based on sarcosine, a metabolite of the amino acid glycine that can be detected in urine [4]. The analytical methods available for direct determination of sarcosine in urine or serum often include chromatography [5–9] and differential mobility analysis [10] with mass spectroscopy. The major disadvantages of these techniques are high instrumentation costs, and complex sample preparation and skilled operator requirements, which is not suitable for routine analysis.

The direct determination of sarcosine may be difficult, but its indirect quantification can be achieved by the reaction between sarcosine and sarcosine oxidase (SOX), which catalyses the oxidative demethylation of sarcosine to glycine, formaldehyde, and hydrogen peroxide. The methods commonly used for the indirect determination of sarcosine are colorimetry [11,12], fluorimetry [13] and electrochemical sensors with immobilization of the enzyme on the electrode surface [14–18]. The enzyme immobilization is a promising choice, due to the intrinsic advantages associated with their high catalytic activity and enzyme specificity for their substrates. The electrode surfaces usually can be mass produced, stored and used as required and in some cases re-used decreasing the cost of the detection process.

In this work, we describe the construction of a novel sarcosine biosensor based on the covalent immobilization of SOX, using *N*-ethyl-*N*-(3-dimethylaminopropyl) carbodiimide (EDC) and *N*-hydroxysuccinimide (NHS), on the surface of the screen-printed carbon electrode. The selectivity of the electrochemical biosensor was improved by covering the electrode surface with Nafion<sup>®</sup>. Nafion is used due to its film hydrophobicity and enzyme-favored environment as well as to enhance selectivity of the sensor by electrostatic repulsion of unwanted species [19,20].

The quantification of sarcosine is achieved herein via electrochemical detection of  $\text{H}_2\text{O}_2$  (Eq. (2)) resulting from the catalyzed oxidation of sarcosine (Eqs. (1) and (2)), i.e., sarcosine oxidase converts sarcosine to glycine, formaldehyde and  $\text{H}_2\text{O}_2$ .



For this purpose, this work presents a systematic investigation study of several experimental parameters. Calibration slopes, dynamic linear range, limit of detection, and selectivity were investigated to evaluate the performance of the sarcosine biosensor for PCa fast and non-invasive screening.

## 2. Experimental procedure

### 2.1. Reagents and solutions

Sarcosine oxidase from *Bacillus* sp (lyophilized powder, 25–50 units/mg), *N*-ethyl-*N*-(3-dimethylaminopropyl) carbodiimide hydrochloride (EDAC), Nafion<sup>®</sup> 117 solution, glutaraldehyde (50%), sodium sulfate, potassium phosphate, ammonium chloride, urea and creatinine were purchased from Sigma–Aldrich. *N*-Hydroxysuccinimide (NHS) was obtained from Fluka; sodium

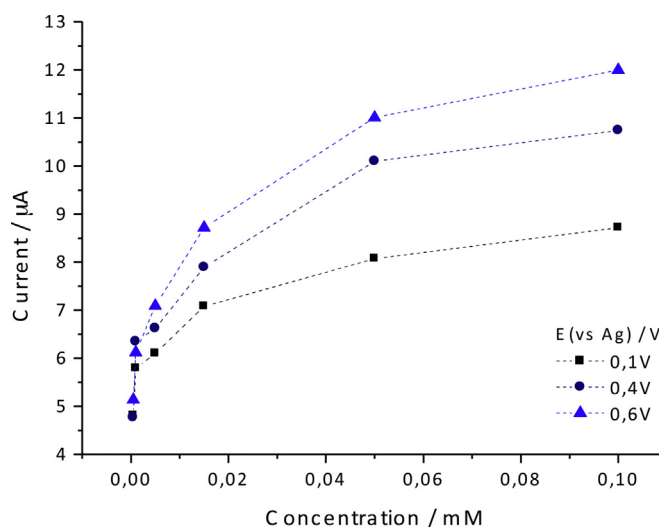


Fig. 1. Calibration curves obtained at different potential values using sensor # 9.

chloride from Panreac; and calcium chloride dihydrate and potassium chloride were obtained from Merck. All the chemicals were of analytical grade and used without further purification.

Phosphate buffer solutions (PBS) at pH 7.2 were used in this work and were prepared with 0.1 M  $\text{NaH}_2\text{PO}_4$  and 0.1 M  $\text{Na}_2\text{HPO}_4$ . Stock solutions of sarcosine ( $C = 1 \times 10^{-3}$  M) were prepared in PBS (pH 7.2) and less concentrated standards were prepared by suitable dilution in the buffer solution. The urine solution used had the following composition: calcium chloride dihydrate ( $1.103 \text{ g L}^{-1}$ ), sodium chloride ( $2.295 \text{ g L}^{-1}$ ), sodium sulfate ( $2.25 \text{ g L}^{-1}$ ), potassium phosphate ( $1.40 \text{ g L}^{-1}$ ), potassium chloride ( $1.60 \text{ g L}^{-1}$ ), ammonium chloride ( $1.00 \text{ g L}^{-1}$ ), urea ( $25 \text{ g L}^{-1}$ ) and creatinine ( $1.10 \text{ g L}^{-1}$ ) [21]. Ultra-pure water (conductivity  $> 18 \text{ M}\Omega \text{ cm}$  at  $25^\circ\text{C}$ ) was used throughout.

### 2.2. Apparatus

The electrochemical measurements were carried out using a potentiostat/galvanostat Autolab Eco Chemie PSTAT10 interfaced to a computer with GPES 4.9 software. Carbon screen-printed electrodes (SPEs, 4 mm diameter, DRP-C110) were used as working electrodes and were purchased from DropSens (Spain). SPEs were

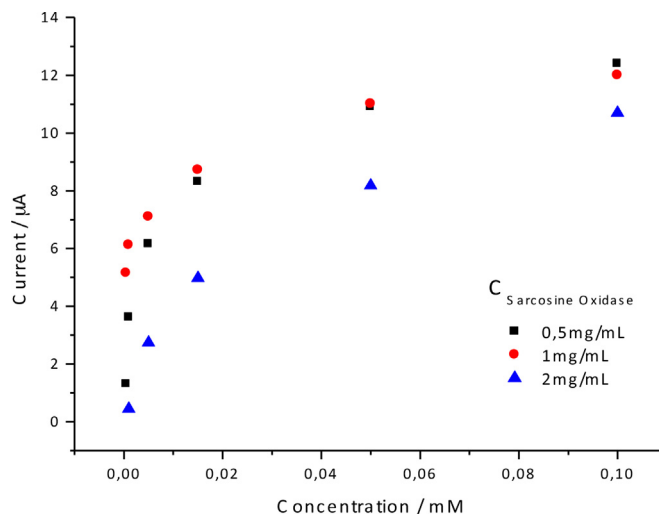
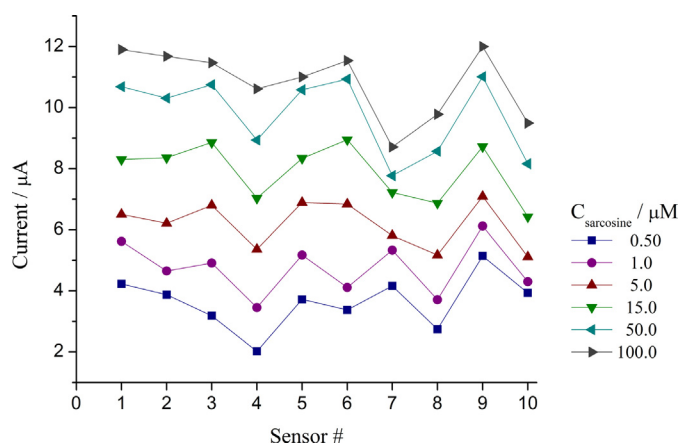


Fig. 2. Calibration curves obtained for different concentration the immobilization of sarcosine oxidase.



**Fig. 3.** Analytical response of the chips fabricated in this work for the increasing concentrations values of sarcosine.

connected to the Autolab by means of a suitable DropSens adaptor box.

Atomic force microscopy (AFM) images were recorded using a Molecular Imaging, PicoLe atomic force microscope. The surface topography was measured using a silicon cantilever/tip (App Nano, model ACT) with a resonance frequency between 200 and 400 kHz.

## 2.3. Procedures

### 2.3.1. Immobilization of sarcosine oxidase

Aiming to choose the best electrode material and the best SOX immobilization procedure a systematic study was carried out using gold and carbon SPE. The results obtained with gold electrode proved not to be satisfactory (the voltammograms were not stable

with signal interferences and therefore higher LOD and reduced linearity was obtained) and this material was discarded in the early stages of this work.

SPE electrodes with carbon films and carbon films containing nanotubes were further tested using different conditions of SOX immobilization with the purpose of increasing enzyme stability and biosensor sensitivity. A summary of the different biosensor configurations studied in this work is presented in Supplementary information, Table S1.

In this paper we describe different immobilization procedures of SOX on the surface of carbon or carbon nanotubes SPE's. The cleaning and oxidation of the carbon electrodes surface was achieved by 30 potential cycles between the potential range from  $-0.2$  to  $+1.0$  V (scan rate:  $100 \text{ mV s}^{-1}$ ) in  $0.5 \text{ M}$  sulfuric acid to ensure that the carboxylic acid groups remain on the surface. The electrodes were then thoroughly rinsed with ultra-pure water and dried under  $\text{N}_2$ .

For the sensors # 1, 2, 8, 9 and 10 (Supplementary information, Table S1), COOH groups were activated by covering the electrode surface with  $5 \mu\text{L}$  of a NHS/EDAC solution ( $10 \text{ mM}$  in PBS) for  $6 \text{ h}$  at room temperature. The reaction of NHS and EDAC at the electrode surface lead to the formation of stable ester surface groups, giving rise to carbon activated surface. The excess of EDAC and NHS was removed by washing the chip with PBS [16]. The COOH groups present in the electrode surfaces of the sensors # 3–7 were not activated.

In the following step, gold (Au) or zinc oxide (ZnO) nanoparticles were used to modify the electrode surfaces by complete evaporation of the aqueous nanoparticles solutions ( $5 \mu\text{L}$ ): sensors 5 and 6 were modified by gold nanoparticles ( $\approx 0.5 \text{ nm}$ ), synthesized by following the protocol of Chirea et al. [22], and sensor # 10 was modified by ZnO ( $\approx 200 \text{ nm}$ ) nanoparticles, synthesized by using the protocol of Jezequel et al. [23]. The electrode surface was washed with PBS to remove the excess of nanoparticles and dried under  $\text{N}_2$ .

The last step of the modification process consists in the immobilization the enzyme sarcosine oxidase (SOX) on the electrode surface by using different immobilization procedures.

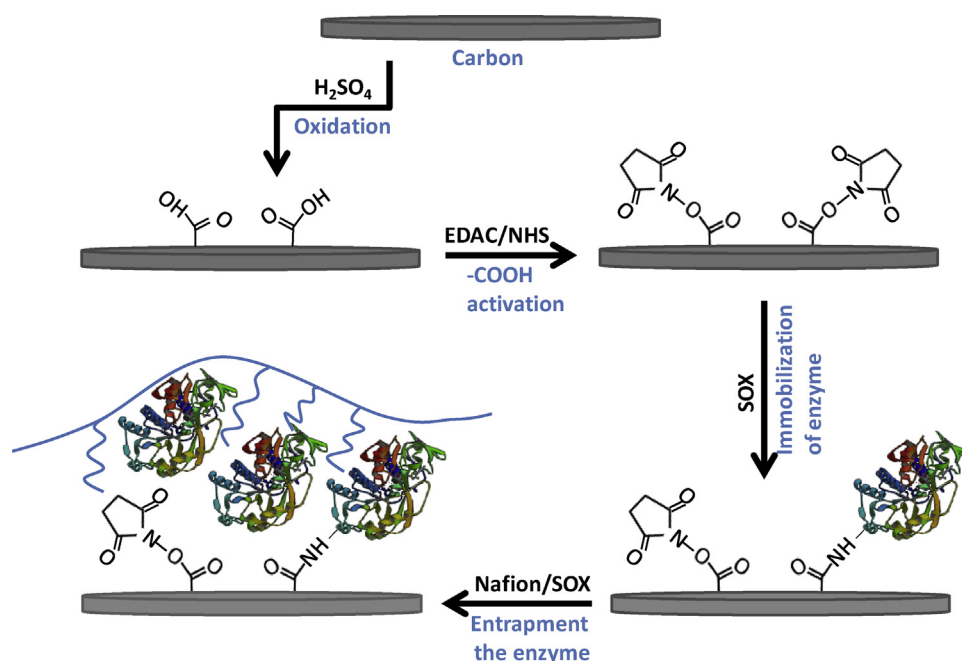


**Fig. 4.** Scheme of the immobilization process of SOX on SPE surface for sensor # 9.

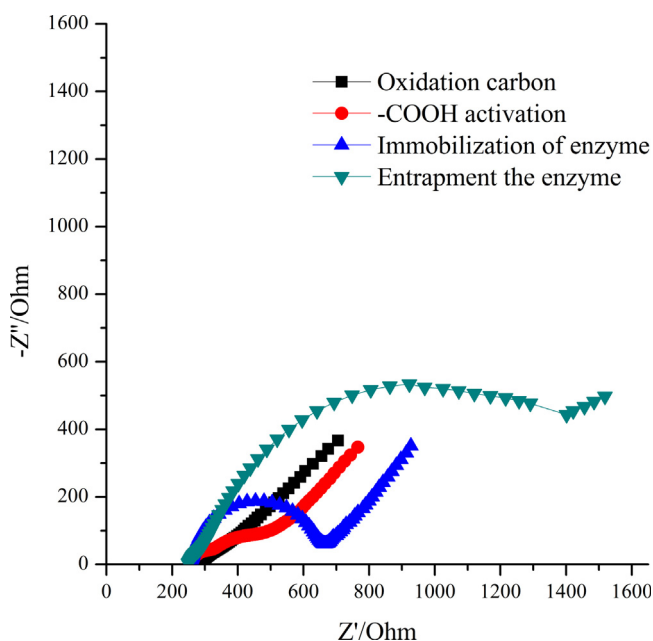


**Fig. 5.** EIS study over the subsequent modification steps of the carbon-SPE in 5.0 mM  $[\text{Fe}(\text{CN})_6]^{3-}$  and 5.0 mM  $[\text{Fe}(\text{CN})_6]^{4-}$  in PBS buffer.

The different electrode surface immobilization processes of SOX are described in Table S1. Electrode surface of sensors # 1, 2 and 9 were modified by depositing 5  $\mu\text{L}$  of SOX solution (1  $\text{mg mL}^{-1}$  in PBS) on the surface of the carbon electrode at 4  $^{\circ}\text{C}$  during 20 h for sensors # 1 and 2 and 6 h for sensor # 9; electrode surface of sensors # 3–6 were modified by dissolving 1 mg SOX in a mixture of 20  $\mu\text{L}$  PBS and 20  $\mu\text{L}$  10% glutaraldehyde. A volume of 5  $\mu\text{L}$  of this solution was applied onto the surface at 4  $^{\circ}\text{C}$  during 20 h [14]; finally, electrode surfaces from sensors # 7–10 were modified by dissolving 1 mg of SOX in a mixture of 20  $\mu\text{L}$  of PBS and 20  $\mu\text{L}$  of Nafion<sup>®</sup> 2.5% [18]. A volume of 5  $\mu\text{L}$  of this solution was applied onto the surface of the electrodes at 4  $^{\circ}\text{C}$  during 20 h. All electrodes were washed with PBS and dried under  $\text{N}_2$ .

### 2.3.2. Electrochemical measurement and optimization of sarcosine biosensor

The sensitivity of sarcosine biosensor was tested by measuring current as function of the applied potential for different solutions with increasing amounts of sarcosine.

Initially 5  $\mu\text{L}$  sarcosine solution ( $5 \times 10^{-6}$ – $3 \times 10^{-1}$  mM in 0.1 M, pH 7.2) was placed at the surface of the sensors and a potential scan was applied using a potential range of  $-1.5$  to  $0.9$  V.

EIS assays were made with redox couple  $[\text{Fe}(\text{CN})_6]^{3-/4-}$  at a potential of  $+0.12$  V, using a sinusoidal potential perturbation with an amplitude of  $0.01$  V and the number of frequencies equal to 50, logarithmically distributed over a frequency range of  $0.1$ – $100$  kHz.

### 2.3.3. Determination of sarcosine in synthetic urine

Synthetic urine solution with different concentrations of sarcosine was used for the evaluation sensor # 9 response. This solution was prepared by adding a known amount of sarcosine (15–65 nM) on to the synthetic urine solution.

## 3. Results and discussions

### 3.1. Optimization of the experimental condition for sarcosine detection

Experiments were carried out using a 0.1 M PBS pH 7.2 as electrolyte solution since it is close to the physiological conditions. In addition, this pH value is within the pH range where sarcosine oxidase has maximum stability (from 7 to 10 in 0.1 M PBS) [24].

The sensitivity of sarcosine biosensor was tested by measuring the current as function of the applied potential (cyclic voltammograms) in the potential range from  $-1.5$  to  $0.9$  V for the different solutions (5  $\mu\text{L}$ ) with increasing concentration of sarcosine (data not shown). The tested sarcosine concentration range was from  $0.5$  to  $100$   $\mu\text{M}$ . The cyclic voltammogram obtained in the absence of sarcosine was used as the baseline in this work.

The optimization of the potential value that corresponds to the maximum current obtained due to  $\text{H}_2\text{O}_2$  oxidation produced by the catalytic decomposition of sarcosine by SOX (Eqs. (1) and (2)) is fundamental to achieve the lowest detection limit and to minimize the interference from other species present in solution. As an example, the current due to the oxidation of  $\text{H}_2\text{O}_2$  for the different concentration of sarcosine was measured for 3 different potentials (0.1, 0.4 and 0.6 V) using sensor # 9, as shown Fig. 1. The current values ( $n=3$ ) were corrected to eliminate the baseline contribution. After analysis of the Fig. 1 it is observed that, although, the steady state current response increased with increasing concentration of sarcosine for the three potentials studied, the potential of 0.6 V was selected because it clearly presented the highest current values, increasing the sensitivity of the sarcosine determination.

The optimization of the effect of sarcosine oxidase concentration on the performance of the sarcosine biosensor was also performed and the results obtained are represented in Fig. 2. Increasing the concentration of sarcosine oxidase as the inconvenience of increasing the cost of the analysis furthermore, from the analysis of data the maximum current obtained is around 20% less than the current obtained using  $1 \text{ mg mL}^{-1}$  of sarcosine oxidase. In addition, the current for the lowest sarcosine concentration tested in this evaluation ( $1 \mu\text{M}$ ) significantly decreases, reducing the linear range of the biosensor response. This may be due to steric effects impairing the interaction between sarcosine and sarcosine oxidase molecules.

Reducing the concentration of sarcosine oxidase to a  $0.5 \text{ mg mL}^{-1}$  level does not change the maximum current obtained however the current for the lowest sarcosine concentration tested in this evaluation ( $1 \mu\text{M}$ ) is lower than that obtained at  $1 \text{ mg mL}^{-1}$  sarcosine oxidase, reducing the linear range of the biosensor response. For those reasons we confirm that the use of  $1 \text{ mg mL}^{-1}$  provides better performance of the biosensor reported in this work (Fig. 3).

**Table 1**  
Fitting parameters extracted from electrochemical impedance data using the Randles equivalent circuit.

|                                 | Oxidation carbon       | COOH activation        | Immobilization of enzyme | Entrapment the enzyme  |
|---------------------------------|------------------------|------------------------|--------------------------|------------------------|
| R ( $\Omega$ )                  | 269.5                  | 259                    | 262                      | 253                    |
| C ( $\mu\text{F}$ )             | 6.32                   | 4.91                   | 1.765                    | 16.95                  |
| $R_{ct}$ ( $\Omega$ )           | 40.5                   | 128.5                  | 368                      | 716                    |
| W ( $\Omega \text{ s}^{-1/2}$ ) | $4.16 \times 10^{-03}$ | $2.50 \times 10^{-03}$ | $2.52 \times 10^{-03}$   | $1.53 \times 10^{-03}$ |

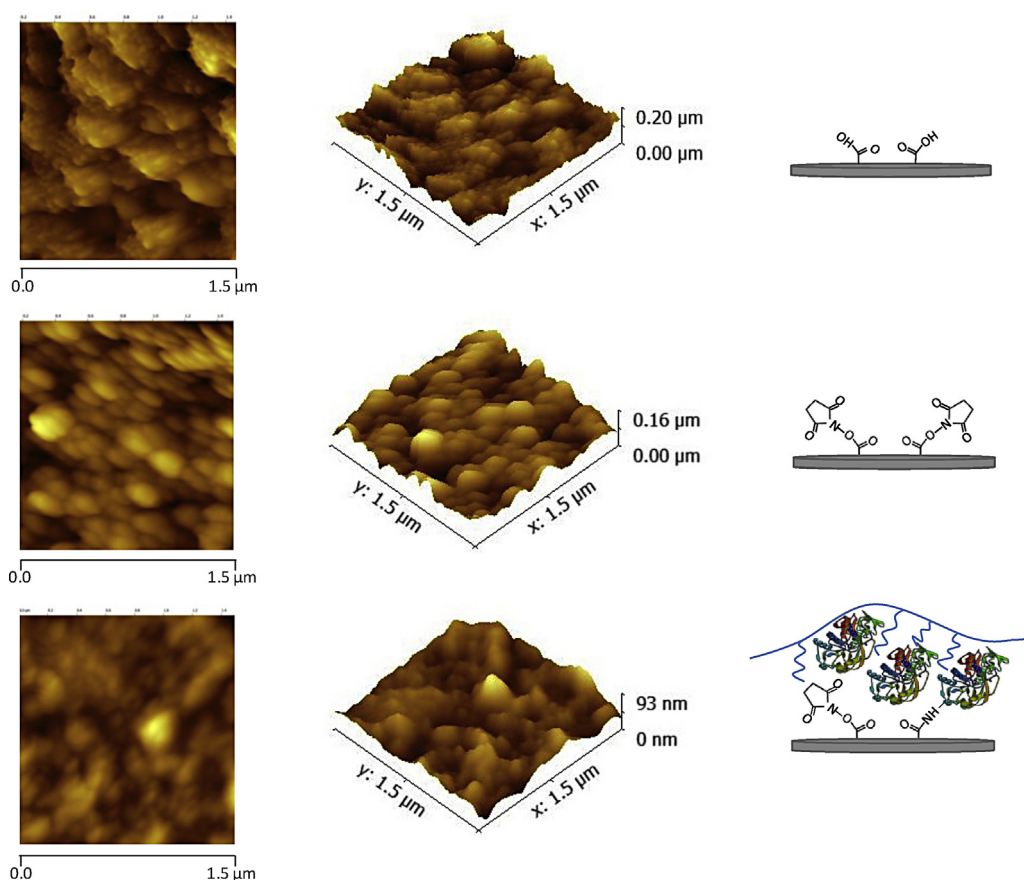


**Fig. 6.** AFM images in 2D (left) and 3D (right) for the different modification of surface SPE electrode.

### 3.2. Optimization of sensor construction method

For the selection of the best sensor fabricated in this work, all sensors were used to measure solutions with different sarcosine concentrations and the results are presented in Fig. 3. As can be

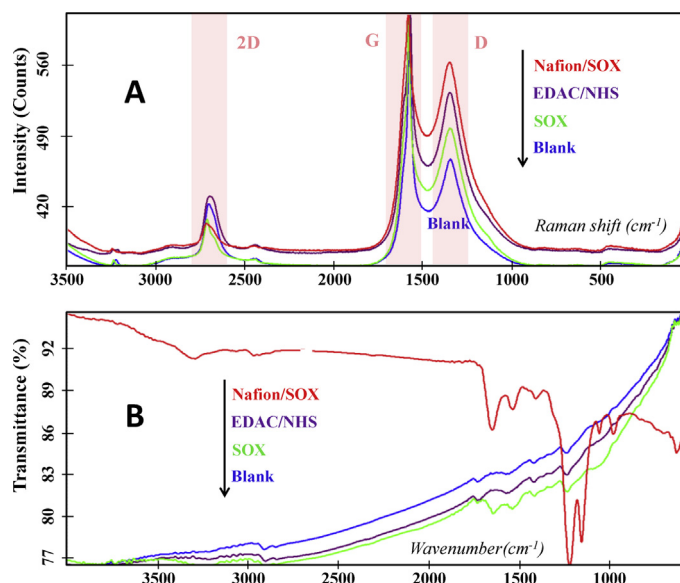


**Fig. 7.** Raman spectroscopy and Fourier transformed infrared spectroscopy (FTIR) analysis.

seen in this figure, sensor # 9 was selected as the best sensor because it presented the highest current values for the same concentration value.

The overall process for the immobilization of SOX on the SPE surface established for sensor # 9 is described in Fig. 4. The first step shows the oxidation of the carbon surface to ensure that the carboxylic acid groups are available at the electrode surface. These groups were then activated via addition of an EDAC/NHS solution and forming ester surface groups, giving rise to a carbon activated surface. In the following step, the enzyme covalent immobilization was achieved by addition of a SOX solution allowing the amine group to react with the ester forming an amide bond, resulting in a covalent immobilization of the enzyme. Finally, a mixture of Nafion and SOX was added in order to entrap the enzyme under a favorable environment where the electrochemical features were simultaneously enhanced.

EIS studies were used to follow the carbon-SPE modification after each chemical change. These can be measured by monitoring the changes in the electron transfer properties of well-known redox systems, such as  $[\text{Fe}(\text{CN})_6]^{4-}/[\text{Fe}(\text{CN})_6]^{3-}$  (Fig. 5).

Results in Fig. 5 clearly show an increase in the resistance of charge transfer when the several sensor layers are built. This reflects the introduction of negative charges at the electrode surface and the increase in the difficulties in the transport of  $[\text{Fe}(\text{CN})_6]^{4-}/[\text{Fe}(\text{CN})_6]^{3-}$  ions toward the electrode surface after the entrapment of the enzyme (this corresponds to the highest increase in charge transfer resistance). Data was fitted to the Randles equivalent circuit in order to extract the numerical values of the charge transfer resistance and those values are displayed in Table 1.



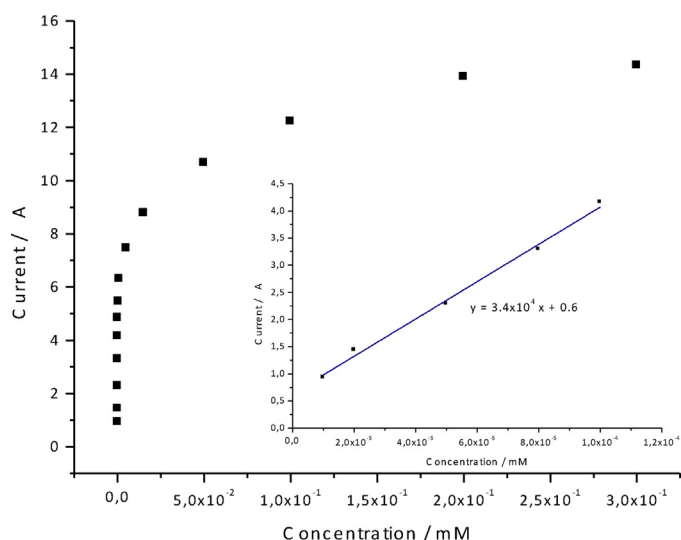


**Fig. 8.** Calibration curve obtained for sarcosine in the concentration range used. Inset: Linear calibration plot obtained for sarcosine.

### 3.3. Surface characterization morphological by AFM, Raman and FTIR

AFM was used to investigate the morphology of the electrode surface before and along the enzyme immobilization process; the images collected are shown in Fig. 6. The top image shows the typical morphology of a clean carbon electrode surface, showing the surface roughness typical of the carbon ink films used in the fabrication of SPEs carbon electrodes.

The root mean square (RMS) surface roughness initially obtained after the oxidation of the carbon at the electrode surface is 27.4 nm (Fig. 6, top) and decreases to 22.1 nm after the activation step of the carboxylic acid groups (Fig. 6, middle). After the last step of the modification procedure, the immobilization and entrapment of enzyme, the RMS value decreases to 12.9 nm (Fig. 6, bottom), indicating that the materials deposit during the successive steps contribute to the decrease the electrodes surface roughness. This can be used as indicative of the success of the immobilization steps.

All chemical modifications made to the carbon electrode were followed by Raman spectroscopy and Fourier transformed infrared spectroscopy (FTIR) analysis. This study was applied to the different stages of the SPE preparation shown in Fig. 4: Blank, EDAC/NHS, SOX and Nafion/SOX. As may be seen in the Raman spectra (Fig. 7A), the relative intensities of the typical G and D peaks of the carbon matrix have changed significantly in all stages of chemical modification. This relative intensity variations account, among others, changes in the ratio of  $sp^2$  and  $sp^3$  carbon hybridization in each staged of the SPE development, therefore confirming the occurrence of chemical change at the working electrode. Regarding the FTIR spectra (Fig. 7B), and as expected, only the presence of Nafion was perceptible above the carbon matrix. The corresponding spectra displayed two strong absorption peaks, at 1153 and 1219  $cm^{-1}$ , typically assigned to the symmetric and asymmetric stretching of  $-CF_2$  groups, respectively [25].

**Table 2**  
Determination of sarcosine in urine samples.

| Sample | Sarcosine (mM)        | Found (mM)                                    | Recovery (%)     | Relative error (%) |
|--------|-----------------------|---|------------------|--------------------|
| 1      | $1.50 \times 10^{-5}$ | $1.82 \times 10^{-5} \pm 3.56 \times 10^{-3}$ | $120.9 \pm 23.7$ | -21.0              |
| 2      | $6.50 \times 10^{-5}$ | $6.75 \times 10^{-5} \pm 4.05 \times 10^{-6}$ | $103.8 \pm 6.23$ | -3.8               |
| 3      | $9.00 \times 10^{-5}$ | $8.50 \times 10^{-5} \pm 3.24 \times 10^{-6}$ | $94.4 \pm 3.60$  | 5.6                |

### 3.4. Evaluation of sarcosine biosensor

After the modification of the electrode surface, the biosensor fabricated was used in the quantification of sarcosine. The hydrogen peroxide generated from the oxidation of sarcosine at the electrode surface ( $E = 0.6$  V) was measured as a function of the sarcosine concentration. The calibration curve obtained is shown in Fig. 8 for the concentration range between 5.0 nM and 0.3 mM. As can be seen in the figure, a saturation of the analytical signal is observed for concentration values greater than 0.1  $\mu$ M which as characteristic of the enzymatic systems. Furthermore, a linear relationship was obtained for sarcosine concentrations ranging from 10 nM to 0.1  $\mu$ M, with a correlation coefficient 0.9966, as shown in the inset of Fig. 8.

The limit of detection (LOD) was calculated according to the Analytical Methods Committee recommendations [26,27] and using a signal-to-noise ratio of 3. An LOD of 16 nM was obtained for the proposed quantification methodology. The LOD obtained in this work is about one order of magnitude lower than the LOD found in the literature for the electrochemical detection of creatinine [15–17]. Comparing to the devices described in the literature for the detection of sarcosine a much higher value is published for the electrochemical device (28  $\mu$ M) [18] and a similar value is found for the optical sensor (5 nM) [12]. However it is important to mention that the optical sensor operates at 37  $^{\circ}C$ , requires sample pre-treatment and cannot be reused.

### 3.5. Interference study and selectivity and electrode stability

Species that coexist with sarcosine in the biological fluids, such as creatinine and/or urea [17], can interfere in the detection of this molecule [7]. The interference study was carried out by comparing the LODs obtained in absence and in the presence of creatinine 1.10  $g L^{-1}$  and urea 25  $g L^{-1}$  [21] and the results obtained are resumed in Supplementary information Table S2. The LODs were estimated from calibration curves obtained in the same linear region. The results obtained indicate that the LODs obtained for sarcosine in the presence of the interferences tested are greater than the obtained for sarcosine in the absence of the interferent which can be explained by the increase of the standard deviation of the baseline (blank solution + interferent  $\times g L^{-1}$ ).

Storage of the biosensor is an important parameter, because the immobilized enzyme on the electrode surface can lose activity. In this work, the biosensor was stored at 4  $^{\circ}C$  and the biosensor could be reused several times ( $\approx 10$ ) with stable results within a period of 60 days. After this period of time, the biosensor performance decreases significantly. When comparing the results obtained for different biosensors prepared using the same immobilization procedure an average relative standard deviation of 2% is found.

### 3.6. Application

Sensor # 9 was applied in the determination of sarcosine in artificial systems with the determination of the molecule in urine samples. Blank samples of synthesized urine were spiked with sarcosine in order to obtain concentrations values ranging from

15 to 65 nM. The results obtained for the three concentration values are summarized in Table 2.

For samples 2 and 3, the recoveries ratios obtained were 103.8% and 94.4%, respectively, corresponding to relative standard deviation errors inferior to 6%. For sample 1, a relative error of 21% was obtained, which can be explained by the fact that the concentration of sarcosine in the urine sample is very close to the LOD of the methodology, increasing the error in the determination of sarcosine.

#### 4. Conclusions

In this study, a simple and low cost electrochemical enzymatic biosensor for the determination of sarcosine in urine, based on the covalent immobilization of SOX, using EDC and NHS, on the surface of the screen-printed carbon electrode has been developed. The biosensor presented high analytical performance features, such as large concentration linear range (10–100 nM), low detection limit (16 nM) and large storage stability (60 days). The biosensor was successfully applied to the analysis of sarcosine in synthetic urine samples.

The proposed detection methodology can be particularly suitable for screening assays carried out in analytical laboratories.

#### Acknowledgements

This work was supported by FCT, Foundation for Science and Technology through the PhD grant ref. SFRH/BD/79221/2011 and CIQUP (Pest-C/QUI/U10081/2013). The authors thank José A. Ribeiro for the constructive discussions and Paula M.V. Fernandes and Inês Miranda for the nanoparticles provided.

#### Appendix A. Supplementary data

Supplementary data associated with this article can be found, in the online version, at <http://dx.doi.org/10.1016/j.aca.2014.08.005>.

#### References

- [1] W.H.O. (WHO), <http://www.who.int/mediacentre/factsheets/fs297/en/index.html> 2008
- [2] N. Cernei, O. Zitka, M. Ryvolova, V. Adam, M. Masarik, J. Hubalek, R. Kizek, Spectrometric and electrochemical analysis of sarcosine as a potential prostate carcinoma marker, *Int. J. Electrochem. Sci.* 7 (2012) 4286–4301.
- [3] E.S. Leman, R.H. Getzenberg, Biomarkers for prostate cancer, *J. Cell. Biochem.* 108 (2009) 3–9.
- [4] A. Sreekumar, L.M. Poisson, T.M. Rajendiran, A.P. Khan, Q. Cao, J. Yu, B. Laxman, R. Mehra, R.J. Lonigro, Y. Li, M.K. Nyati, A. Ahsan, S. Kalyana-Sundaram, B. Han, X. Cao, J. Byun, G.S. Omenn, D. Ghosh, S. Pennathur, D.C. Alexander, A. Berger, J. R. Shuster, J.T. Wei, S. Varambally, C. Beecher, A.M. Chinnaiyan, Metabolomic profiles delineate potential role for sarcosine in prostate cancer progression, *Nature* 457 (2009) 910–914.
- [5] T.E. Meyer, S.D. Fox, H.J. Issaq, X. Xu, L.W. Chu, T.D. Veenstra, A.W. Hsing, A reproducible and high-throughput HPLC/MS method to separate sarcosine from  $\alpha$ - and  $\beta$ -alanine and to quantify sarcosine in human serum and urine, *Anal. Chem.* 83 (2011) 5735–5740.
- [6] C. Burton, S. Gamagedara, Y. Ma, Partial enzymatic elimination and quantification of sarcosine from alanine using liquid chromatography–tandem mass spectrometry, *Anal. Bioanal. Chem.* 405 (2013) 3153–3158.
- [7] Y. Jiang, X. Cheng, C. Wang, Y. Ma, Quantitative determination of sarcosine and related compounds in urinary samples by liquid chromatography with tandem mass spectrometry, *Anal. Chem.* 82 (2010) 9022–9027.
- [8] F. Bianchi, S. Dugheri, M. Musci, A. Bonacchi, E. Salvadori, G. Arcangeli, V. Cupelli, M. Lanciotti, L. Masieri, S. Serni, M. Carini, M. Careri, A. Mangia, Fully automated solid-phase microextraction – fast gas chromatography – mass spectrometry method using a new ionic liquid column for high-throughput analysis of sarcosine and *N*-ethylglycine in human urine and urinary sediments, *Anal. Chim. Acta* 707 (2011) 197–203.
- [9] H. Wu, T. Liu, C. Ma, R. Xue, C. Deng, H. Zeng, X. Shen, GC/MS-based metabolomic approach to validate the role of urinary sarcosine and target biomarkers for human prostate cancer by microwave-assisted derivatization, *Anal. Bioanal. Chem.* 401 (2011) 635–646.
- [10] P. Martínez-Lozano, J. Rus, Separation of isomers  $\alpha$ -alanine and sarcosine in urine by electrospray ionization and tandem differential mobility analysis–mass spectrometry, *J. Am. Soc. Mass Spectrom.* 21 (2010) 1129–1132.
- [11] C.S. Pundir, N. Chauhan, G.K. Vandana, Immobilization of *Arthrobacter* sarcosine oxidase onto alkylamine and arylamine glass and its application in serum sarcosine determination, *Indian J. Biotechnol.* 10 (2011) 219–223.
- [12] J. Lan, W. Xu, Q. Wan, X. Zhang, J. Lin, J. Chen, J. Chen, Colorimetric determination of sarcosine in urine samples of prostatic carcinoma by mimic enzyme palladium nanoparticles, *Anal. Chim. Acta* 825 (2014) 63–68.
- [13] C. Burton, S. Gamagedara, Y. Ma, A novel enzymatic technique for determination of sarcosine in urine samples, *Anal. Methods* 4 (2012) 141–146.
- [14] A. Ramanavicius, Amperometric biosensor for the determination of creatine, *Anal. Bioanal. Chem.* 387 (2007) 1899–1906.
- [15] S. Yadav, R. Devi, P. Bhar, S. Singha, C.S. Pundir, Immobilization of creatininase, creatinase and sarcosine oxidase on iron oxide nanoparticles/chitosan-g-polyaniline modified Pt electrode for detection of creatinine, *Enzyme Microb. Technol.* 50 (2012) 247–254.
- [16] S. Yadav, A. Kumar, C.S. Pundir, Amperometric creatinine biosensor based on covalently coimmobilized enzymes onto carboxylated multiwalled carbon nanotubes/polyaniline composite film, *Anal. Biochem.* 419 (2011) 277–283.
- [17] C.-H. Chen, M.S. Lin, A novel structural specific creatinine sensing scheme for the determination of the urine creatinine, *Biosens. Bioelectron.* 31 (2012) 90–94.
- [18] P. Kotzian, N.W. Beyene, L.F. Llano, H. Moderegger, P. Tunón-Blanco, K. Kalcher, K. Vytras, Amperometric determination of sarcosine with sarcosine oxidase entrapped with nafion on manganese dioxide-modified screen-printed electrodes, scientific papers of the University of Pardubice, Serie A Faculty Chem. Technol. 8 (2002) 93–101.
- [19] L. Mao, F. Xu, Q. Xu, L. Jin, Miniaturized amperometric biosensor based on xanthine oxidase for monitoring hypoxanthine in cell culture media, *Anal. Biochem.* 292 (2001) 94–101.
- [20] A.C. Torres, M.E. Ghica, C.A. Brett, Design of a new hypoxanthine biosensor: xanthine oxidase modified carbon film and multi-walled carbon nanotube/carbon film electrodes, *Anal. Bioanal. Chem.* 405 (2013) 3813–3822.
- [21] C.J. Collins, A. Berduque, D.W.M. Arrigan, Electrochemically modulated liquid–liquid extraction of ionized drugs under physiological conditions, *Anal. Chem.* 80 (2008) 8102–8108.
- [22] M. Chirea, E.M. Pereira, C.M. Pereira, F. Silva, Synthesis of poly-lysine/gold nanoparticle films and their electrocatalytic properties, *Biointerf. Res. Appl. Chem.* 1 (2011) 119–126.
- [23] D. Jezequel, J. Guenot, N. Jouini, F. Fievet, Submicrometer zinc oxide particles: elaboration in polyol medium and morphological characteristics, *J. Mater. Res.* 10 (1994) 77–83.
- [24] Y. Matsuda, H. Hoshika, Y. Inouye, S. Ikuta, K. Matsuura, S. Nakamura, Purification and characterization of sarcosine oxidase of *Bacillus* origin, *Chem. Pharmaceut. Bull.* 35 (1987) 711–717.
- [25] L. Grosmaire, S. Castagnoni, P. Huguet, P. Sistat, M. Boucher, P. Bouchard, P. Bébin, S. Deabate, Probing proton dissociation in ionic polymers by means of in situ ATR-FTIR spectroscopy, *Phys. Chem. Chem. Phys.* 10 (2008) 1577–1583.
- [26] Analytical Methods Committee, Recommendations for the definition, estimation and use of the detection limit, *Analyst* 112 (1987) 199–204.
- [27] J. Mocak, A.M. Bond, S. Mithell, G. Scollary, A statistical overview of standard (IUPAC and ACS) and new procedures for determining the limits of detection and quantification: application to voltammetric and stripping techniques. Technical report, *Pure Appl. Chem.* 69 (1997) 297–328.